



# An emergent constraint on Transient Climate Response from simulated historical warming in CMIP6 models

Femke J.M.M. Nijssse<sup>1</sup>, Peter M. Cox<sup>1</sup>, and Mark S. Williamson<sup>1</sup>

<sup>1</sup>University of Exeter, College of Engineering, Mathematics and Physical Sciences, EX4 4QE, Exeter, UK

**Correspondence:** Femke J.M.M. Nijssse (f.j.m.m.nijssse@exeter.ac.uk)

**Abstract.** The transient climate response (TCR) is the metric of temperature sensitivity that is most relevant to warming in the next few decades, and contributes the biggest uncertainty to estimates of the carbon budgets consistent with the Paris targets (Arora et al., 2019). In the IPCC 5th Assessment Report (AR5), the stated ‘likely’ range of TCR was given as 1.0 to 2.5 K, with a central estimate which was broadly consistent with the ensemble mean of the CMIP5 Earth System Models (ESMs) available at the time ( $1.8 \pm 0.4$  K). Many of the latest CMIP6 ESMs have larger climate sensitivities, with 6 of 23 models having TCR values above 2.5 K, and an ensemble mean TCR of  $2.1 \pm 0.4$  K. On the face of it, these latest ESM results suggest that the IPCC likely range of TCR may need revising upwards, which would cast further doubt on the feasibility of the Paris targets. Here we show that rather than increasing the uncertainty in climate sensitivity, the CMIP6 models help to further constrain the likely range of TCR to 1.5-2.2 K, with a central estimate of 1.82 K. We reach this conclusion through an emergent constraint approach which relates the value of TCR to the global warming from 1970 onwards. We confirm a consistent emergent constraint on TCR when we apply the same method to CMIP5 models (Jiménez-de-la Cuesta and Mauritsen, 2019). Our emergent constraint on TCR benefits from both the large range of TCR values across the CMIP6 models, and also from the extension of the historical simulations into a period when the uncertain changes in aerosol forcing have had a far less significant impact on the trend in global warming.

## 1 Introduction

The key uncertainty in projections of future climate change continues to be the sensitivity of global mean temperature to perturbations of the Earth’s energy budget, normally termed ‘radiative forcing’. This sensitivity is usually characterised in terms of the global mean temperature that would occur if the atmospheric carbon dioxide concentration was doubled, for which the radiative forcing is reasonably well-known.

Two related parameters are used to characterise the climate sensitivity of Earth System Models (ESMs). Equilibrium Climate Sensitivity (ECS) is an estimate of the eventual steady-state global warming at double  $\text{CO}_2$ . Transient Climate Response (TCR) is the mean global warming predicted to occur around the time of doubling  $\text{CO}_2$  in ESM runs for which atmospheric  $\text{CO}_2$  concentration is prescribed to increase at 1% per year. Across an ensemble of ESMs, TCR values are typically around half of ECS values because of ocean heat uptake, which leads to a lag in the response of global temperature to the increasing  $\text{CO}_2$  concentration.



Despite significant advances in climate science, both ECS and TCR remain uncertain. The ‘likely’ range of ECS (66% confidence limit) has been quoted as 1.5 K to 4.5 K in all of the five Assessment Reports (ARs) of the Intergovernmental Panel on Climate Change (IPCC) starting in 1990, aside from the AR4 which moved the likely lower range temporarily to 2 K. Similarly the likely range of TCR is given as 1 K to 2.5 K in the IPCC AR5, based on multiple lines of evidence.

30 There have been numerous attempts to constrain ECS using the record of historical warming or palaeoclimate data (Knutti et al., 2017), and more recently using emergent constraints which relate observed climate trends or variations to ECS using an ensemble of models (Caldwell et al., 2018; Cox et al., 2018a). However, debate still rages about the likely range of ECS (Brown et al., 2018; Po-Chedley et al., 2018; Rypdal et al., 2018; Cox et al., 2018b), in part because observed global warming is a rather indirect measure of global warming at equilibrium. On the other hand, TCR is more closely related to the rate of  
35 warming, and therefore ought to be more amenable to constraint by the record of global warming (Jiménez-de-la Cuesta and Mauritsen, 2019). Nevertheless, the accepted likely range of TCR has also resisted change (Knutti et al., 2017), for reasons we will discuss in this paper. At the time of the AR5, the CMIP5 ESMs produced central estimates (mean  $\pm$  stdev) of ECS ( $3.2 \pm 0.7$  K) and TCR ( $1.8 \pm 0.4$  K), that were consistent with these IPCC likely ranges. However, there has been a general drift upwards towards higher climate sensitivities in the new CMIP6 ESMs, such that almost half of the new CMIP6 models now  
40 have ECS values over 4.5 K (Forster et al., 2019), and more than a quarter have TCR values over 2.5 K (Table 1). If the real climate system is similarly sensitive, the Paris climate targets will be much harder to achieve.

Therefore some key policy-relevant questions arise:

- (a) *Are such high climate sensitivities consistent with the observational record?*
- (b) *If so, do the CMIP6 models demand an upward revision to the IPCC likely ranges for climate sensitivity?*

45 We address these questions in this paper by evaluating the historical simulations of global warming from the CMIP6 models. In particular, we explore an emergent constraint on TCR based on global warming from 1970 onwards (Jiménez-de-la Cuesta and Mauritsen, 2019), but using the CMIP6 models and observational data up to 2018.

Emergent constraints are increasingly used to assess future change by exploiting statistical relationships in multimodel ensembles between an observable and a variable describing future climate (Cox et al., 2018a; Hall et al., 2019). In the work  
50 presented here, we use the latest CMIP6 multimodel ensemble to define an emergent relationship between historical warming (the observable) and TCR (the variable describing future climate). In line with published recommendations (Hall et al., 2019; Klein and Hall, 2015), we check the robustness of the resulting emergent constraint against the CMIP5 ensemble, using exactly the same methodology as for CMIP6. We also follow the suggestion of Hall et al. (2019) in striving to base our emergent constraint on sound physical reasoning, as outlined below.

55 By definition, we expect values of TCR to be very well-correlated with simulated global warming across a model ensemble, if all models are driven by a 1.0% per year increase in CO<sub>2</sub>. These are the idealised conditions used to estimate TCR, so only internal variability would deny a perfect correlation between TCR and the modelled rate of global warming in this case. However, historical global warming has not been driven by a 1.0% per year CO<sub>2</sub> increase, but instead by a smaller near-exponential rate of CO<sub>2</sub> increase (0.5% per year since 2000 (Dlugokenchy and Tans, 2019)), augmented by additional positive



60 radiative forcing from other well-mixed greenhouse gases (especially methane and nitrous oxide), and partially offset by the cooling effects of anthropogenic aerosols.

The radiative effects of the known increases in greenhouse gas concentrations are relatively well-known (Myhre et al., 2013), and are broadly similar in different ESMs. By contrast, the radiative forcing due to changes in anthropogenic aerosols, especially indirect effects via changes in cloud brightness and lifetime, are poorly constrained (Myhre et al., 2013).

65 These uncertainties in aerosol forcing have hindered attempts to constrain TCR from the rate of warming, especially during the pre-1980 period when the burning of sulphurous coal led to increases in CO<sub>2</sub> and increases in sulphate aerosols, that went up almost together (Andreae et al., 2005). As a result it has been difficult to distinguish, based purely on the observational record of global warming, between a model with high TCR and strong aerosol cooling, and a model with low TCR and weak aerosol cooling.

70 In order to minimise the effects of uncertainties in aerosol forcing, we need periods in which aerosol radiative forcing changes relatively little compared to the change in radiative forcing due to CO<sub>2</sub> and other well-mixed greenhouse gases. Fortunately, this applies to the decade after 1970 when total aerosol load from global SO<sub>2</sub> and NH<sub>3</sub> emissions were similar to values over the last decade (Stevens et al., 2017). For this reason, we follow Jiménez-de-la Cuesta and Mauritsen (2019) in focusing on global warming since 1970. However, in addition we explore a range of start and finish dates to assess the robustness of our  
75 TCR constraint, and to test the hypothesis that the relationship between TCR and warming rate is emerging strongly now because of the declining importance of changes in aerosol forcing.

The remainder of this paper is organised as follows: in Section 2 we describe our methodological choices; Section 3 contains the emergent constraint on TCR and Section 4 contains the discussion and conclusions. More technical details concerning the regression methods are given in the Appendix.

## 80 2 Method

We use the CMIP6 multimodel ensemble to find an emergent relationship between historical warming and TCR. We use all currently available models that have control (piControl), historical, Shared Socioeconomic Pathway 3-7.0 (ssp370) and one percent CO<sub>2</sub> increase per year (1pctCO2) experiments. From the 1pctCO2 experiment TCR is determined as the average temperature difference from the corresponding piControl run between 60 to 80 years after the start of the simulation. Values  
85 of TCR are given in table 1. Historical warming (our observable) is found from the historical and ssp370 simulations using the global annual mean surface air temperature (GMSAT) smoothed with a centred running mean. Some of these models have multiple runs starting from different initial conditions, forcing time series or parameter settings. We use all available runs. This results in a set of 95 simulations from 13 different models.

We use smoothed GMSAT to calculate warming. This is to limit the random effect of internal variability on the forced change  
90 we wish to constrain. We choose a centred 11-year running mean to remove shorter interannual and mid-term variability from sources such as ENSO, as well as reducing the effect of longer period modes of natural variability. We have tested the robustness



**Table 1.** List of CMIP6 models used in this study and their equilibrium climate sensitivity (ECS) and transient climate response (TCR). Mean values are reported for models with multiple realisations. ECS and the climate feedback parameter  $\lambda$  are computed using the Gregory method (Gregory, 2004). Starred models had full model output available and are the ones included in the emergent constraint. Values for CMIP5 are from (Flato et al., 2013), and model selection the same as in (Nijssen et al., 2019).

Centre	Model	$F_{2xCO_2}$ ( $W m^{-2}$ )	$\lambda$ ( $W m^{-2} K^{-1}$ )	ECS (K)	TCR (K)
*BCC	BCC-CSM2-MR	3.01	0.98	3.07	1.59
BCC	BCC-ESM1	3.03	0.93	3.35	1.76
*CAMS	CAMS-CSM1-0	3.39	1.76	2.35	1.75
*CCCma	CanESM5	3.63	0.64	5.66	2.66
*CNRM CERFACS	CNRM-CM6-1	3.54	0.72	4.94	2.08
*CNRM CERFACS	CNRM-ESM2-1	3.09	0.66	4.66	1.92
E3SM Project	E3SM-1.0	3.23	0.60	5.38	2.99
*EC Earth Consortium	EC-Earth3-Veg	3.32	0.77	4.34	2.57
*IPSL	IPSL-CM6A-LR	3.32	0.72	4.63	2.32
*MIROC	MIROC6	3.75	1.47	2.56	1.52
*MIROC	MIROC-ES2L	-	-	-	1.55
MOHC	HadGEM3-GC31-LL	3.39	0.62	5.52	2.52
*MOHC	UKESM1-0-LL	3.56	0.66	5.41	2.72
*MRI	MRI-ESM2-0	3.36	1.07	3.14	1.56
NASA GISS	GISS-E2-1-G	3.89	1.44	2.70	1.72
NASA GISS	GISS-E2-1-H	3.54	1.17	3.09	1.89
*NCAR	CESM2	3.12	0.63	5.17	2.08
*NCAR	CESM2-WACCM	3.08	0.69	4.90	1.92
NCC	NorESM2-LM	-	-	-	1.46
NOAA GFDL	GFDL-CM4	2.90	0.71	4.09	1.97
NUIST	NESM3	-	-	-	2.73
SNU	SAM0-UNICON	3.85	1.06	3.67	2.18
UA	MCM-UA-1.0	-	-	-	1.94
	<b>CMIP6 mean</b>	3.40 (3.42*)	0.90 (*0.89)	4.16 (*4.24)	2.06 (*2.01)
	<b>CMIP6 standard deviation</b>	0.32 (0.35*)	0.33 (*0.35)	1.09 (*1.11)	0.44 (*0.42)
	<b>CMIP5 mean</b>	3.44	1.19	3.04	1.83
	<b>CMIP5 standard deviation</b>	0.46	0.31	0.72	0.38



of our constraint on TCR to the length of the running mean. It remains relatively invariant past a length of 5 years suggesting most of the internal variability in GMSAT resides in shorter periods.

Warming  $\Delta T$  is calculated as the difference in smoothed GMSAT between two periods, typically the years 1970-1980 and 2008-2018. We have chosen the end year to be 2018 to maximise the chances of discrimination between high and low sensitivity models i.e. as the forcing from  $\text{CO}_2$  increases with time, the warming in more sensitive models is more likely diverge from less sensitive ones resulting in stronger statistical relationships between TCR and  $\Delta T$ . Although we use 2018 as the end year of annual GMSAT, we report the central year of the smoothed timeseries in the following figures i.e. the central year of annual GMSAT smoothed with a centred running mean of 11 years would be shown as 2013.

Other reasons for choosing 2018 include being able to use the most recent observational data and to eliminate possible effects from the warming slowdown between 2000-2012. This slowdown has been attributed to a combination of internal variability and decreased forcing, amongst other things (Medhaug et al., 2017). We have investigated whether this reduced forcing makes a difference to our emergent constraint by extending the historical CMIP6 simulations from 2014 to 2018 using the SSP scenario simulations. The different SSP scenarios have very similar greenhouse gas emissions for the 2015-2019 period, and the choice of SSP does not significantly alter our findings. We use SSP3-7.0 as this SSP has the largest number of model simulations at the time of writing. Choosing either 2014 or 2018 does not significantly affect our results.

We have chosen the starting period to be 1970-1980 when aerosols forcing was similar to today's values. This choice also minimised the uncertainty in our estimate of TCR. As a function of start period, uncertainty is relatively flat and minimal between periods with central years of 1975 and 1985.

Once choices of length of running mean and start and end years for calculation of  $\Delta T$  are fixed (our observable), we can fit an emergent relationship between the observable and our values of TCR via linear regression. Linear regression is performed using a hierarchical Bayesian model which can take into account all the different simulations per model: models with more simulations have a better-constrained post-aerosol warming. The regression method is further described in Appendix A.

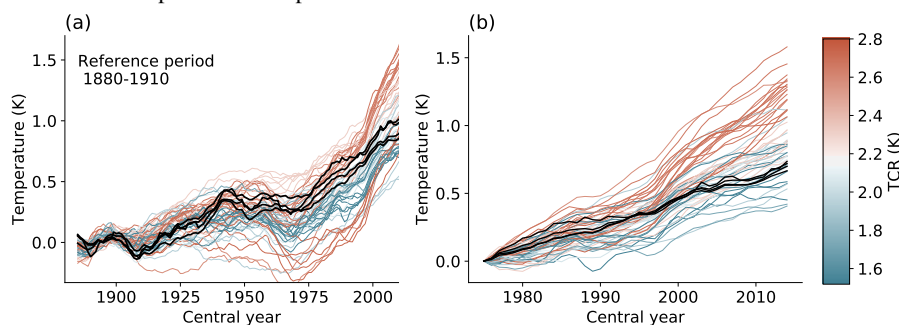
### 3 Results

Figure 1a shows the  $\Delta T$  over the period 1880 to 2018 simulated by 13 different CMIP6 models running a total of 95 simulations smoothed with a 11-year running mean relative to the mean of the reference period 1880-1910. Model runs have been colour coded by their TCR, darker red indicating models with higher TCR, darker blue indicating lower TCR. Black lines are various observational datasets of the same period. Models with higher TCR either show large  $\Delta T$  at the end of the period, or portray a strong aerosol cooling over the 20th century, particularly visible as a dip around 1970 (notably CNRM-ESM1, UKESM1-0-LL and EC-Earth-Veg). The major uncertainty for historical radiative forcing comes from aerosols (Bellouin et al., 2019). Figure 1b shows the same information for the end of the historical period although the reference period is now chosen to be 1970-1980, close to the dip. The positive correlation intuitively expected between TCR and  $\Delta T$  is more clearly seen.

The  $\Delta T$  for each model simulation in Fig. 1b is used in our emergent constraint on TCR in Fig. 2a. Observational warming (black vertical dashed line) is the mean of HadCRUT4 (Morice et al., 2012), Berkeley Earth (Rohde et al., 2013), GISTEMP4



**Figure 1.** Global mean surface temperature of 13 individual CMIP6 models named in Table 1. An 11-year running mean was used. (a)  $\Delta T$  using the mean GMSAT between 1880-1910 as reference period. (b)  $\Delta T$  relative to the 1970-1980 mean. To avoid overrepresenting a single model, a maximum of ten realisations per model are plotted.



125 (Lenssen et al., 2019) and NOAA v5 (Zhang et al., 2019). The confidence interval (grey shaded vertical area) is a combination  
of the observational uncertainty and the internal variability. The models from the previous CMIP5 generation generally fall  
within the prediction interval of the CMIP6 emergent constraint: the emergent constraint is robust across generations (Klein  
and Hall, 2015). The best estimate (1.82 K) from this emergent constraint is very similar to the best estimate using the larger  
set of models that have historical simulations up to 2014, but no future scenarios (1.77 K, [1.31 - 2.22 K, likely range]). The set  
130 of CMIP6 models used in our emergent constraint are listed in table 1 along with their TCR and ECS values, the latter being  
determined from Gregory plots (Gregory, 2004) on the first 150 year of the abrupt-4xCO<sub>2</sub> simulations.

Figure 2b shows the probability density functions (pdf) of TCR derived from the emergent constraint for both CMIP6 and  
the earlier CMIP5 model ensembles. For comparison, the raw model range in each CMIP is plotted as a histogram, as well as  
the reported IPCC AR5 range. The IPCC pdf is not specified, here we take it as a normal distribution. Both CMIP5 and CMIP6  
135 pdfs are very similar (central estimates differ by 0.05 K) even though raw model means in CMIP6 and CMIP5 differ by 0.23 K.  
As a continuation of the historical CMIP5 simulation, RCP4.5 is chosen.

### 3.1 Robustness to parameter choices

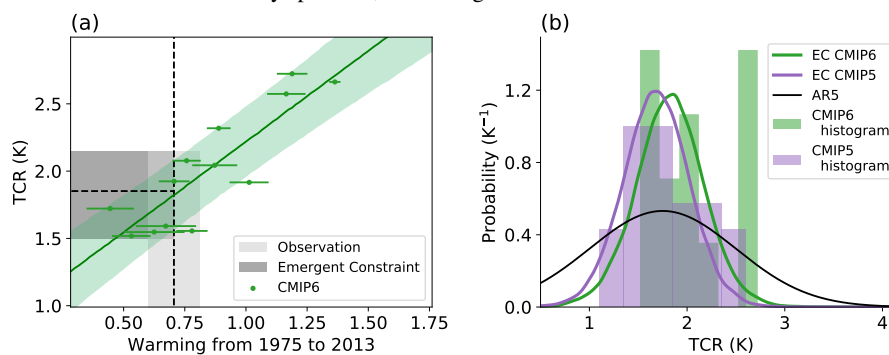
We have assessed how robust our estimate of TCR is to the various choices of parameters:

#### 3.1.1 End year

140 Estimates of TCR depend on the final year chosen for the emergent constraint. However, uncertainty in the estimate of TCR  
reduces as time increases and the central estimate converges as shown in Figure 3a. Later end years are intuitively preferred  
(i.e. 2018) as the increased CO<sub>2</sub> forcing with time leads to more separation in models warming predictions over their internal  
variability. This increases correlation of warming with TCR and reduces uncertainty in the best estimate. We believe this might  
also be due to the reducing relative effect of aerosol forcing compared to forcing from CO<sub>2</sub> at later years.



**Figure 2.** (a) Emergent constraint on TCR against historical warming  $\Delta T$ .  $\Delta T$  is calculated from the difference between 1970-1980 and 2008-2018 of a timeseries of GMSAT smoothed with a centred 11 year running mean, denoted by their central year on axis label. Linear regression is performed with all CMIP6 simulations. Shaded areas indicate a 66% confidence interval (see Appendix A). The vertical dotted line is the mean value of the observations and the horizontal dotted line is the implied central estimate of the TCR. (b) Comparison of probability distributions for the transient climate response using post-1970 warming using CMIP5 and CMIP6 simulations. The probability distribution in the fifth IPCC assessment is not fully specified, and the figure shows a normal distribution with the same likely range as IPCC.



### 145 3.1.2 Length of running mean

To mitigate the effect of internal variability, we use a running mean of GMSAT. Figure 3b shows the likely range of TCR as a function of the length of the running mean. Since we use all available simulations including multiple realisations of the same model in our emergent constraint, the effect of internal variability is already reduced and the length of the running mean on the estimate of TCR is small - the central estimate and the likely range remain relatively invariant past a length of 5 years.

### 150 3.1.3 Start year

Figure 3c shows the effect of the start year on the emergent constraint. Uncertainty in the estimated value of TCR is minimal and relatively flat between start years of 1975 and 1985. Uncertainty from start years of 1985 onwards increases although slowly until the estimate and the uncertainty revert towards the raw CMIP6 ensemble statistics (no predictive power) at later years.

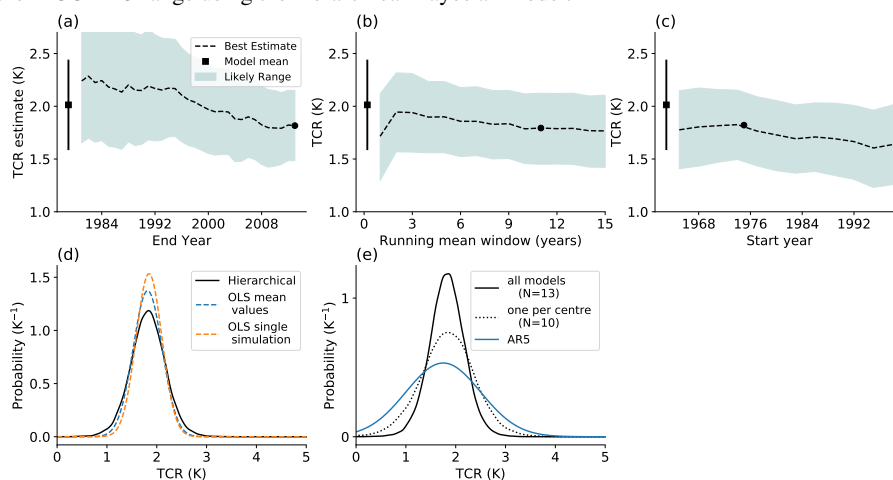
### 155 3.1.4 Regression method

When only one realisation per model is used for ordinary least square regression, regression dilution takes place in which the slope is underestimated (Cox et al., 2018b). This leads to a slight overestimation of TCR (Figure 3d), as the observed warming is on the lower end of model warming. Jiménez-de-la Cuesta and Mauritsen (2019) used the average warming for models with multiple simulations. As not all models provide (a sufficient amount) of simulations, they state that this leads to a minor inflation of the estimation of uncertainty. Although we use a hierarchical Bayesian model as the default (details in Appendix A)





**Figure 3.** Robustness of the result to various parameter choices and the choice of regression method. Unless stated differently, start year is 1975, all years up to 2018 are used, and the length of the running mean is 11 years. **(a)** Likely TCR range as a function of the end year (dotted line central estimate). **(b):** Likely TCR range as a function of length of running mean. **(c)** Likely TCR range as a function of start year. **(d)** Pdf of TCR from different regression methods: the hierarchical Bayesian model is compared to three other linear regression methods used in the emergent constraint literature: ordinary least squares (OLS) with only one realisation per model, OLS on the mean warming per model and orthogonal distance regression (ODR). **(e)** Resulting pdfs on TCR from stricter model selection (one model per modelling centre) compared to the all models and the IPCC AR5 range using the hierarchical Bayesian model.



we have investigated two other regression methods used in the emergent constraint literature: ordinary least squares (OLS) with only one realisation per model and OLS on the mean warming per model Fig. 3d. All give very similar results.

### 3.1.5 Model selection

It has been noted that model selection can prevent double counting of very similar models (Sanderson et al., 2015; Cox et al., 2018a). As models from the same centre can have very dissimilar climate sensitivities (Chen et al., 2014; Jiménez-de-la Cuesta and Mauritsen, 2019) and sensitivity can change drastically with only small adjustments to parameters (Zhao et al., 2016), we use all available models in the CMIP5 and CMIP6 ensemble. Figure 3e shows that this choice does not significantly change the best estimate of the transient response, but using all models gives a stronger constraint.

## 4 Discussion and Conclusion

170 An immediate question that may come to mind after constraining TCR, is whether the same information can be used to constrain ECS. There is an approximately linear relationship between ECS and TCR across the CMIP6 ensemble, but this shows significant scatter due to variation in ocean heat uptake across the ensemble (see Figure 4). As a result, although our central estimate of TCR corresponds to ECS values slightly over 3K, some models with ECS > 4.5 K also fall within the





likely bounds of our TCR constraint. We find no good evidence to support a particular non-linear relationship between ECS  
175 and TCR (Rugenstein et al., 2019), and therefore little evidence of a direct emergent constraint on ECS from recent warming  
alone (Jiménez-de-la Cuesta and Mauritsen, 2019). In the future, we hope that our TCR constraint will become the basis for  
constraints also on ECS and TCRE (Transient Climate Response to Emissions), but this will require the inclusion of additional  
constraints on ocean heat uptake, and land and ocean carbon uptake, respectively.

However, we are now in a position to answer the questions that we posed in Section 1, at least with regard to TCR:

180 (a) *Are such high climate sensitivities consistent with the observational record?*

No, models with high TCR ( $>2.5$  K) are not consistent with observed global warming since 1970, as demonstrated in  
Figure 1b.

(b) *If so, do the CMIP6 models demand an upward revision to the IPCC likely ranges for climate sensitivity?*

Our associated emergent constraint on TCR (Figure 2) does not warrant a revision upwards of the IPCC likely range for  
185 TCR, despite the larger TCR values in the CMIP6 ensemble.

Instead, the CMIP6 models help to constrain the likely TCR range, without significantly changing the central estimate. Our  
best estimate for TCR from the CMIP6 models is 1.82K, which remains close to the centre of the likely range (1-2.5K) given in  
the IPCC AR5 (IPCC, 2013). The emergent constraint on TCR from the CMIP6 models is however strong enough to indicate  
a much tighter likely range of TCR (1.5-2.2K).

190 We find a consistent emergent constraint from the CMIP5 models against observed global warming from 1970 to 2018  
(1.31-2.22 K). Furthermore, both of these likely ranges overlap strongly with the emergent constraint on TCR derived by  
(Jiménez-de-la Cuesta and Mauritsen, 2019) using a similar method, but only considering global warming from 1970 to 2005  
(1.17-2.16 K). In terms of the classification proposed by Hall et al. (2019), we therefore now have a *confirmed* emergent  
constraint on TCR, implying an approximate likely range of 1.5 to 2.2K.

195 *Code availability.* The code to analyse the data and produce the figures is available upon request to the corresponding author.

*Data availability.* CMIP5 and CMIP6 data can be accessed through ESGF nodes.

## Appendix A: Hierarchical linear regression

To systematically include the information from all model realisations, we use a hierarchical Bayesian model (Sansom, 2014).  
This model includes two layers: the normal linear regression and a layer that computes the expected warming per model from  
200 all its initial value realisations. To include the initial value ensemble, we assume that each model  $i$  has a "true" or "best" value  
for warming over the last decades denoted by  $\Delta T_T$ . We further assume that every realisation  $j$  of a model gives a value of

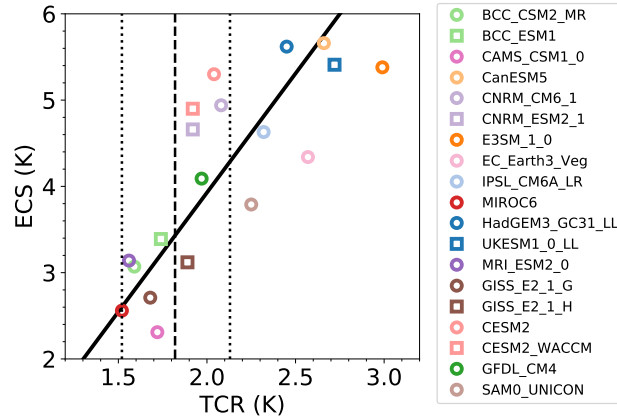


**Figure 4.** Scatter plot of TCR values plotted against ECS values for all CMIP6 models with both available at the time of submission. Models from the same modelling group are plotted with the same colour. Plot markers differentiate models from the same modelling centre. Regression line computed with orthogonal distance regression (ODR).

$\Delta T$  that is drawn from a normal distribution with mean  $\Delta T_T$  and a standard deviation  $\sigma_x$  that is the same across all models. Our hierarchical model consists of two steps: for each model the best estimate of historical warming is computed and with this value a simple linear regression is performed:

```

205   for( $j$  in 1: $N$ ){
            $\Delta T_{all}[j] \sim \text{normal}(\Delta T_T[j], \sigma_x);$ 
       }
       for( $i$  in 1: $N_g$ ){
            $\text{TCR}[i] \sim \text{normal}(\alpha + \beta \Delta T_T[i], \sigma_y);$ 
210   }
    
```

The probability density function is then sampled from the observation of warming between 1970 and 2018  $\overline{\Delta T}$  and the emergent constraint. The observational uncertainty  $\sigma_{obs}$  is taken as the sample standard deviation of the four observational datasets.

$$\text{TCR}_{pred} = \text{normal}_{\text{rng}}(\alpha + \beta \text{normal}_{\text{rng}}(\overline{\Delta T}, \sqrt{\sigma_x^2 + \sigma_{obs}^2}), \sigma_y);$$

Here `rng` is a (pseudo) random number generator. The second for loop corresponds with normal linear regression, while  
 215 the first for loop makes an estimate of the true  $\Delta T_T$ . Note that for models with only few initial value member, the "best"  $\Delta T_T$  does not necessarily correspond with that the value of this only ensemble member.



Weakly informative priors are chosen for the intercept  $\alpha$ , the slope  $\beta$ , the uncertainty of the regression  $\sigma_y$  and the internal variability  $\sigma_x$ :

$$\begin{aligned} \alpha &\sim \text{normal}(0, 5); \\ 220 \quad \beta &\sim \text{normal}(0, 10); \\ \sigma_y &\sim \text{half-normal}(0.5, 10); \\ \sigma_x &\sim \text{half-normal}(0.2, 0.5); \end{aligned}$$

*Author contributions.* All authors contributed towards the design of the study. MSW led on the data collection, FJMMN led on the data analysis with contributions from MSW and PMC. All authors contributed equally to the manuscript.

225 *Competing interests.* The authors declare no competing interests.

*Acknowledgements.* This work was supported by the European Research Council ECCLES project, grant agreement number 742472 (F.J.M.M.N., P.M.C. and M.S.W.); the EU Horizon 2020 Research Programme CRESCENDO project, grant agreement number 641816 (P.M.C. and M.S.W.). We also acknowledge the World Climate Research Programme's Working Group on Coupled Modelling, which is responsible for CMIP, and we thank the climate modelling groups (listed in Table 1) for producing and making available their model output.



## 230 References

- Andreae, M. O., Jones, C. D., and Cox, P. M.: Strong present-day aerosol cooling implies a hot future, <https://doi.org/10.1038/nature03671>, <http://www.nature.com/articles/nature03671>, 2005.
- Arora, V. K., Katavouta, A., Williams, R. G., Jones, C. D., Brovkin, V., Friedlingstein, P., Schwinger, J., Bopp, L., Boucher, O., Cadule, P., Chamberlain, M. E., Christian, J. R., Delire, C., Fischer, R. A., Hajima, T., Ilyina, T., Joetzjer, E., Kawamiya, M., Koven, C., Krasting, J.,  
235 Law, R. M., Lawrence, D. M., Lenton, A., Lindsay, K., Pongratz, J., Raddatz, T., Séférian, R., Tachiiri, K., Tjiputra, J. F., Wiltshire, A., Wu, T., and Ziehn, T.: Carbon-concentration and carbon-climate feedbacks in CMIP6 models, and their comparison to CMIP5 models, *Biogeosciences Discussions*, 2, 2019.
- Bellouin, N., Quaas, J., Gryspeerdt, E., Kinne, S., Stier, P., Watson-Parris, D., Boucher, O., Carslaw, K., Christensen, M., Daniau, A., Dufresne, J., Feingold, G., Fiedler, S., Forster, P., Gettelman, A., Haywood, J., Malavelle, F., Lohmann, U., Mauritsen, T., Mc-  
240 Coy, D., Myhre, G., Mühlmenstädt, J., Neubauer, D., Possner, A., Rugenstein, M., Sato, Y., Schulz, M., Schwartz, S., Sourdeval, O., Storelvmo, T., Toll, V., Winker, D., and Stevens, B.: Bounding aerosol radiative forcing of climate change, *Reviews of Geophysics*, <https://doi.org/10.1029/2019RG000660>, 2019.
- Brown, P. T., Stolpe, M. B., and Caldeira, K.: Assumptions for emergent constraints, *Nature*, 563, E1–E3, <https://doi.org/10.1038/s41586-018-0638-5>, <http://www.nature.com/articles/s41586-018-0638-5>, 2018.
- 245 Caldwell, P. M., Zelinka, M. D., and Klein, S. A.: Evaluating Emergent Constraints on Equilibrium Climate Sensitivity, *Journal of Climate*, <https://doi.org/10.1175/JCLI-D-17-0631.1>, <https://journals.ametsoc.org/doi/pdf/10.1175/JCLI-D-17-0631.1>, <http://journals.ametsoc.org/doi/10.1175/JCLI-D-17-0631.1>, 2018.
- Chen, X. L., Zhou, T. J., and Guo, Z.: Climate sensitivities of two versions of FGOALS model to idealized radiative forcing, *Science China Earth Sciences*, 57, 1363–1373, <https://doi.org/10.1007/s11430-013-4692-4>, 2014.
- 250 Cox, P. M., Huntingford, C., and Williamson, M. S.: Emergent constraint on equilibrium climate sensitivity from global temperature variability, *Nature*, 553, 319–322, <https://doi.org/10.1038/nature25450>, <http://www.nature.com/doi/10.1038/nature25450>, 2018a.
- Cox, P. M., Williamson, M. S., Nijssen, F. J. M. M., and Huntingford, C.: Cox et al. reply, *Nature*, 563, E10–E15, <https://doi.org/10.1038/s41586-018-0641-x>, <http://www.nature.com/articles/s41586-018-0641-x>, 2018b.
- Dlugokenchy, E. and Tans, P.: Trends in Atmospheric Carbon Dioxide, [https://www.esrl.noaa.gov/gmd/ccgg/trends/gl\\_gr.html](https://www.esrl.noaa.gov/gmd/ccgg/trends/gl_gr.html), 2019.
- 255 Flato, G., Marotzke, J., B. Abiodun, P. B., Chou, S., Collins, W., Cox, P., Driouech, F., Emori, S., Eyring, V., Forest, C., Gleckler, P., Guilyardi, E., Jakob, C., Kattsov, V., Reason, C., and Rummukainen, M.: Evaluation of Climate Models, in: *Climate Change 2013: The Physical Science Basis. Contribution of Working Group I to the Fifth Assessment Report of the Intergovernmental Panel on Climate Change*, edited by Stocker, T., D. Qin, G.-K. P., Tignor, M., Allen, S., J. Boschung, A. N., Xia, Y., Bex, V., and (eds.), P. M., Cambridge University Press, Cambridge, United Kingdom and New York, NY, USA, 2013.
- 260 Forster, P. M., Maycock, A. C., McKenna, C. M., and Smith, C. J.: Latest climate models confirm need for urgent mitigation, *Nature Climate Change*, pp. 1–4, <https://doi.org/10.1038/s41558-019-0660-0>, <http://www.nature.com/articles/s41558-019-0660-0>, 2019.
- Gregory, J. M.: A new method for diagnosing radiative forcing and climate sensitivity, *Geophysical Research Letters*, 31, L03 205, <https://doi.org/10.1029/2003GL018747>, <http://doi.wiley.com/10.1029/2003GL018747>, 2004.
- Hall, A., Cox, P., Huntingford, C., and Klein, S.: Progressing emergent constraints on future climate change, *Nature Climate Change*, 9,  
265 269–278, <https://doi.org/10.1038/s41558-019-0436-6>, <http://www.nature.com/articles/s41558-019-0436-6>, 2019.



- IPCC: Climate Change 2013: The Physical Science Basis. Contribution of Working Group I to the Fifth Assessment Report of the Intergovernmental Panel on Climate Change, Cambridge University Press, Cambridge, United Kingdom and New York, NY, USA, <https://doi.org/10.1017/CBO9781107415324>, [www.climatechange2013.org](http://www.climatechange2013.org), 2013.
- Jiménez-de-la Cuesta, D. and Mauritsen, T.: Emergent constraints on Earth's transient and equilibrium response to doubled CO<sub>2</sub> from post-1970s global warming, *Nature Geoscience*, 12, 902–905, <https://doi.org/10.1038/s41561-019-0463-y>, <http://www.nature.com/articles/s41561-019-0463-y>, 2019.
- Klein, S. A. and Hall, A.: Emergent Constraints for Cloud Feedbacks, *Current Climate Change Reports*, 1, 276–287, <https://doi.org/10.1007/s40641-015-0027-1>, 2015.
- Knutti, R., Rugenstein, M. A., and Hegerl, G. C.: Beyond equilibrium climate sensitivity, <https://doi.org/10.1038/NGEO3017>, <http://www.nature.com/articles/ngeo3017>, 2017.
- Lenssen, N., Schmidt, G., Hansen, J., Menne, M., Persin, A., Ruedy, R., and Zyss, D.: Improvements in the GISTEMP uncertainty model, *J. Geophys. Res. Atmos.*, 124, 6307–6326, <https://doi.org/10.1029/2018JD029522>, 2019.
- Medhaug, I., Stolpe, M. B., Fischer, E. M., and Knutti, R.: Reconciling controversies about the 'global warming hiatus', *Nature*, 545, 41–47, <https://doi.org/10.1038/nature22315>, <http://www.nature.com/doi/10.1038/nature22315>, 2017.
- Morice, C. P., Kennedy, J. J., Rayner, N. A., and Jones, P. D.: Quantifying uncertainties in global and regional temperature change using an ensemble of observational estimates: The HadCRUT4 data set, *Journal of Geophysical Research: Atmospheres*, 117, <https://doi.org/10.1029/2011JD017187>, <https://agupubs.onlinelibrary.wiley.com/doi/abs/10.1029/2011JD017187>, 2012.
- Myhre, G., Shindell, D., Bréon, F.-M., W. Collins, J. F., Huang, J., Koch, D., J.-F. Lamarque, D. L., Mendoza, B., Nakajima, T., Robock, A., Stephens, G., Takemura, T., and Zhang, H.: Anthropogenic and Natural Radiative Forcing, in: *Climate Change 2013: The Physical Science Basis. Contribution of Working Group I to the Fifth Assessment Report of the Intergovernmental Panel on Climate Change*, edited by Stocker, T., D. Qin, G.-K. P. Tignor, M., Allen, S., J. Boschung, A. N., Xia, Y., Bex, V., and (eds.), P. M., Cambridge University Press, Cambridge, United Kingdom and New York, NY, USA, 2013.
- Nijse, F. J., Cox, P. M., Huntingford, C., and Williamson, M. S.: Decadal global temperature variability increases strongly with climate sensitivity, *Nature Climate Change*, 9, 598–601, <https://doi.org/10.1038/s41558-019-0527-4>, <http://www.nature.com/articles/s41558-019-0527-4>, 2019.
- Po-Chedley, S., Proistosescu, C., Armour, K. C., and Santer, B. D.: Climate constraint reflects forced signal, *Nature*, 563, E6–E9, <https://doi.org/10.1038/s41586-018-0640-y>, <http://www.nature.com/articles/s41586-018-0640-y>, 2018.
- Rohde, R., Muller, R., Jacobsen, R., Perlmutter, S., and Mosher, S.: Berkeley Earth Temperature Averaging Process, *Geoinformatics & Geostatistics: An Overview*, 01, <https://doi.org/10.4172/2327-4581.1000103>, 2013.
- Rugenstein, M., Bloch-Johnson, J., Gregory, J., Mauritsen, T., Li, C., Frölicher, T., Danabasoglu, G., Yang, S., Dufresne, J.-L., Schmidt, G. A., Abe-Ouchi, A., and Geoffroy, O.: Equilibrium climate sensitivity estimated by equilibrating climate models 2, Submitted, <https://doi.org/10.1029/2019GL083898>, 2019.
- Rypdal, M., Fredriksen, H. B., Rypdal, K., and Steene, R. J.: Emergent constraints on climate sensitivity, *Nature*, 563, E4–E5, <https://doi.org/10.1038/s41586-018-0639-4>, <http://www.nature.com/articles/s41586-018-0639-4>, 2018.
- Sanderson, B. M., Knutti, R., and Caldwell, P.: A representative democracy to reduce interdependency in a multimodel ensemble, *Journal of Climate*, <https://doi.org/10.1175/JCLI-D-14-00362.1>, 2015.
- Sansom, P. G.: Statistical methods for quantifying uncertainty in climate projections from ensembles of climate models, Ph.D. thesis, University of Exeter, <https://ore.exeter.ac.uk/repository/handle/10871/15292>, 2014.



- 305 Stevens, B., Fiedler, S., Kinne, S., Peters, K., Rast, S., Müsse, J., Smith, S. J., and Mauritsen, T.: MACv2-SP: A parameterization of anthropogenic aerosol optical properties and an associated Twomey effect for use in CMIP6, *Geoscientific Model Development*, 10, 433–452, <https://doi.org/10.5194/gmd-10-433-2017>, 2017.
- Zhang, H.-M., Huang, B., Lawrimore, J., Menne, M., and Smith, T. M.: Global Surface Temperature Dataset (NOAAGlobalTemp), Version 5.0, <https://doi.org/10.7289/V5FN144H>, 2019.
- 310 Zhao, M., Golaz, J. C., Held, I. M., Ramaswamy, V., Lin, S. J., Ming, Y., Ginoux, P., Wyman, B., Donner, L. J., Paynter, D., and Guo, H.: Uncertainty in model climate sensitivity traced to representations of cumulus precipitation microphysics, *Journal of Climate*, 29, 543–560, <https://doi.org/10.1175/JCLI-D-15-0191.1>, 2016.